Proc. Natl. Acad. Sci. USA
Vol. 96, pp. 7520–7525, June 1999
Neurobiology

Relationship between presynaptic calcium transients and postsynaptic currents at single γ-aminobutyric acid (GABA)ergic boutons

S. KIRISCHUK, N. VESELOVSKY, AND R. GRANTYN*

Arbeitsgruppe Entwicklungsphysiologie, Institut für Physiologie, Medizinische Fakultät (Charité) der Humboldt-Universität zu Berlin, 10117 Berlin, Germany

Edited by Per O. Andersen, University of Oslo, Oslo, Norway, and approved April 9, 1999 (received for review November 2, 1998)

ABSTRACT **Postsynaptic responses to stereotyped activation of single axons are known to fluctuate, but the origin of synaptic variability in the vertebrate central nervous system is still unclear. To test the hypothesis that fluctuations of inhibitory postsynaptic currents reflect variations in presynaptic Ca^{2+} concentration, we examined single GABAergic axodendritic contacts in low-density cultures. Collicular neurons from rat embryos were loaded with the Ca^{2+} indicator Oregon Green 488 BAPTA-1. Presynaptic axon terminals were visualized by staining with the styryl dye RH414. Under the condition of action potential block, RH414-labeled boutons were activated selectively by current pulses applied through a fine-tipped glass pipette. Short (1- to 3-ms) depolarization of isolated boutons resulted in stimulus-locked changes of presynaptic Ca^{2+} concentration ($[Ca^{2+}]_{pre}$) and in evoked inhibitory postsynaptic currents (eIPSCs). Varying the strength of the stimulating currents produced a wide amplitude range of both presynaptic fluorescence transients (up to 220% of the resting value) and postsynaptic conductance changes (up to 2–3 nS). It was found that average eIPSCs displayed an approximately third-power dependency on $[Ca^{2+}]_{pre}$. Transmitter release retained its probabilistic character throughout the range of observed $[Ca^{2+}]_{pre}$ values. In any tested single bouton, maximal eIPSCs occurred in association with the largest $[Ca^{2+}]_{pre}$ transients, but failures were present at any $[Ca^{2+}]_{pre}$. The increase of maximal eIPSC amplitudes in connection with higher $[Ca^{2+}]_{pre}$ supports the hypothesis that GABAergic boutons have the capacity to regulate synaptic strength by changing the number of simultaneously released vesicles.**

Transmitter release is triggered by a localized elevation of concentration in a specialized area called the "active zone," where transmitter-containing vesicles and Ca^{2+} channels are clustered together (1). Most of what is known about the relationship between presynaptic Ca^{2+} influx and postsynaptic responses is derived from especially large synapses with multiple active zones. In the squid giant synapse (2, 3) and in the neuromuscular junction (4–8), postsynaptic responses were recorded in parallel with presynaptic Ca^{2+} currents or changes in the presynaptic Ca^{2+} concentration ($[Ca^{2+}]_{pre}$). These and other studies (reviewed in refs. 9–11) showed that the release-associated changes in $[Ca^{2+}]_{pre}$ are very local, large, and rapid. Ca^{2+} influx creates microdomains of elevated $[Ca^{2+}]_{pre}$ in the immediate vicinity of Ca^{2+} channels. At the inner-channel face, $[Ca^{2+}]_{pre}$ could reach hundreds of micromoles per liter. The very small distance between the channel mouth and the release site, together with the requirement for high $[Ca^{2+}]$, is thought to account for both the fast initiation and termination of release. In addition, it was shown that the relationship between the postsynaptic response and the presynaptic Ca^{2+} influx is highly nonlinear (4, 6, 12).

The latter conclusion was extended to a giant synapse in the vertebrate central nervous system (CNS) (13). Despite the fact that synapses in the mammalian CNS are commonly formed by small axon varicosities that comprise not more than one to two active zones (14, 15), it became possible to examine some of them in the slice by recording whole-cell or field excitatory postsynaptic currents in their dependency on pooled $[Ca^{2+}]_{pre}$ (16). A third- to fourth-power function described the dependency of excitatory postsynaptic currents on $[Ca^{2+}]_{pre}$ in excitatory axon terminals of the cerebellum and hippocampus (17, 18), and it was shown that this relationship was strongly dependent on the type of Ca^{2+} channel involved (17).

Fluorescent markers allowed identification of the site of vesicle accumulation in axon terminals (19), providing an opportunity to study evoked transmitter release from individual synapses in low-density dissociated cell cultures. In a first series of experiments, inhibitory synaptic currents were elicited in the presence of a Na^+-channel blocker by direct depolarization of single FM1–43-stained boutons (20). This activation technique was introduced by Katz and Miledi (21) and used later by a number of other investigators (22, 23). In comparison with single-bouton activation by local application of concentrated KCl (24, 25) or sucrose solution (26, 27), the method of direct electrical stimulation has the advantage that the range of $[Ca^{2+}]_{pre}$ could be expanded by precise gradation of presynaptic depolarization. Deficits in the control over the presynaptic membrane potential may be compensated partly by the availability of $[Ca^{2+}]_{pre}$ as an indicator for presynaptic activation. In this way, postsynaptic fluctuations can be studied in activity-matched samples.

Fluctuations in synaptic transmission are thought to contribute to the functional adjustment in neuronal networks (28). However, little still is known about the mechanisms underlying the stochastic nature of communication between neurons. In the CNS, action potential (AP)-mediated synaptic transmission is not very reliable. It can fail for a variety of reasons, including alteration of AP duration, conduction failure, reduced transmitter storage, vesicle depletion, decrease of Ca^{2+} influx, changes in Ca^{2+} buffering, or postsynaptic receptor desensitization. By analyzing, at the level of single boutons, the variability of individual $[Ca^{2+}]_{pre}$ in conjunction with the corresponding postsynaptic responses, it might be possible to identify sources of transmission failure downstream of the Ca^{2+} influx. Finally, evaluating the relationship between evoked inhibitory postsynaptic current (eIPSC) amplitudes

The publication costs of this article were defrayed in part by page charge payment. This article must therefore be hereby marked "*advertisement*" in accordance with 18 U.S.C. §1734 solely to indicate this fact.

PNAS is available online at www.pnas.org.

This paper was submitted directly (Track II) to the *Proceedings* office.
Abbreviations: $[Ca^{2+}]$, Ca^{2+} concentration; $[Ca^{2+}]_{pre}$, presynaptic $[Ca^{2+}]$; AP, action potential; CNS, central nervous system; eIPSC, evoked inhibitory postsynaptic current; GABA, γ-aminobutyric acid; Org1, Oregon Green 488 1,2-bis(2-aminophenoxy)ethane-*N,N,N′,N′*-tetraacetate acetoxymethyl ester.

*To whom reprint requests should be sent at: AG Entwicklungsphysiologie, Institut für Physiologie der Charité, Tucholskystrasse 2, D-10117 Berlin. e-mail: rosemarie.grantyn@charite.de.

and $[Ca^{2+}]_{pre}$ could help to clarify the conditions for multivesicular release and to estimate the number of simultaneously releasing vesicles as a potentially important variable of synaptic strength at the level of single γ-aminobutyric acid (GABA)ergic synapses.

The present experiments were aimed at answering the following questions. Do postsynaptic responses continue to fluctuate if a single bouton is activated in a controlled manner? And, if so, do the postsynaptic current amplitudes vary in dependence on $[Ca^{2+}]_{pre}$?

MATERIALS AND METHODS

Preparation. Superior colliculi of embryonic day 21 Wistar rats were removed, dissociated, and plated as described in Perouansky and Grantyn (29), except that cells were seeded at a lower density (75,000 cells per cm^2), on laminin-coated glass coverslips. Antimitotics were not used. Cultures were studied between 10 and 36 days *in vitro*, when neuron densities amounted to $8–10 \times 10^3$ per cm^2.

Imaging. Cultures first were loaded with Oregon Green 488 1,2-bis(2-aminophenoxy)ethane-*N,N,N′,N′*-tetraacetate acetoxymethyl ester (Org1; 5 μM, 15–20 min at 36°C) and then kept in standard salt solution (SSS; 140 mM NaCl/3 mM KCl/1 mM $MgCl_2$/1.5 mM $CaCl_2$/20 mM Hepes·NaOH/30 mM glucose, pH 7.4) for an additional 20 min to ensure deesterification. After that, synaptic vesicles were stained with RH414 by using a two-step procedure. After incubation (15–20 s) in high-potassium (30 mM) salt solution containing 50 μM RH414, cultures were kept for 30 s in the SSS containing the same concentration of the dye. After that the cells were washed twice with the SSS. The coverslip with the stained cultures formed the bottom of a recording chamber on the stage of an inverted microscope (Axiovert 100; Zeiss). A ×100 phase-contrast objective (Zeiss) was used to select axodendritic contacts for imaging and stimulation. Excitation wavelength was controlled by a fast monochromator system, and fluorescent signals were recorded by a charge-coupled device (CCD) camera (TILL Photonics, Planegg, Germany). Numerically, one pixel of this CCD camera collected the light from a 0.1×0.1-μm area in the focal plane. All measurements were performed by using 4×4 binning (0.4×0.4 μm). The acquisition rate for $[Ca^{2+}]$ measurement was one image per 10 ms. The probes were excited at 490 nm. The excitation and emission light was separated by using a 510-nm dichroic mirror. The emitted light was filtered at 550 ± 30 nm for Org1 and at 600 nm for RH414. Several phase-contrast images and an RH414 image were captured at the beginning of each experiment. The RH414 image was binarized at a threshold of half-maximal intensity above the background and used as a mask (by multiplication) to define the region of interest (ROI) for subsequent Org1 images. Thus, the presynaptic ROIs represented the area of vesicle accumulation. The background fluorescence originating from glial cells was calculated from a region in the immediate vicinity of the stimulated bouton and subtracted. To decrease contamination of the ROI signal by fluorescence from the underlying dendrite, all measurements were performed after at least 15 min of postsynaptic neuron dialysis. Moreover, the postsynaptic cell then was depolarized to 0 mV for 1 s. When the fluorescence change in the presynaptic ROI exceeded 10% of the resting value, the experiment was discontinued. This test will be referred to as "dendritic Ca^{2+} test." Fluorescence signals were expressed as relative changes from prestimulus levels ($\Delta F/F_0$). For simplicity, $\Delta F/F_0$ also will be referred to as $[Ca^{2+}]_{pre}$.

Stimulation and Recording. Glass stimulation pipettes filled with SSS (8–12 MΩ) were placed close to an RH414-labeled spot. An isolated stimulation unit was used to generate electrical stimuli. Unless otherwise stated, boutons were activated at 0.1 or 0.2 s^{-1} by applying depolarizing pulses for 1–3 ms. Stimulating currents (0.5–1.5 μA) were recorded throughout. Whole-cell patch clamp recordings were performed by using glass pipettes containing 100 mM potassium gluconate/50 mM KCl/5 mM NaCl/2 mM $MgCl_2$/1 mM $CaCl_2$/10 mM EGTA/20 mM Hepes·KOH, pH 7.2. E_{Cl} was about −20 mV. Signals were acquired at 10 kHz by using a conventional patch clamp amplifier and acquisition software (EPC-7 or EPC-8 with TIDA 3.0; HEKA Electronics, Lambrecht/Pfalz, Germany). Series resistance (10–12 MΩ) was compensated up to 70–75%. Stimulus-related capacitance artifacts were subtracted by using averaged failure traces. The time course of postsynaptic depolarization resulting from imperfect voltage control ("voltage escape") was determined by estimating the changes in the driving force for eIPSCs after the pulse. The relaxation time constant measured during the peak of an eIPSC was less than 3 ms. When short stimuli (1–3 ms) were used, eIPSCs started after the pulse, and peak amplitudes were underestimated by no more then 5%.

Superfusion. All experiments were performed at room temperature (23–25°C). A slow superfusion system was used. The flow rate was 0.5 ml/min. To test the effect of Ca^{2+}-free or bicuculline-containing solution, a glass superfusion pipette (40-μm tip diameter) was placed at a distance of about 50 μm. Ca^{2+}-free solution contained 2.5 mM $MgCl_2$, no added $CaCl_2$, and no EGTA. Tetrodotoxin (1 μM), 6,7-dinitroquinoxaline-2,3-dione (10 μM), and DL-2-amino-5-phosphonopentanoic acid (50 μM) were added to the SSS to prevent AP generation and glutamatergic synaptic transmission. Org1 and RH414 were obtained from Molecular Probes, and all other chemicals were from Sigma.

RESULTS

The culture conditions favored the formation of GABAergic synaptic connections (30). Nevertheless, postsynaptic currents were identified as IPSCs by their sensitivity to bicuculline, slow time course, and reversal at chloride equilibrium potential. Well isolated axon terminals located at the side of a first-order dendrite were best suited for the present experiments (Fig. 1*A*). In terms of bouton size, our sample is representative of previously described immunolabeled GABAergic boutons in collicular cultures (31). The bouton projection on the dendrite

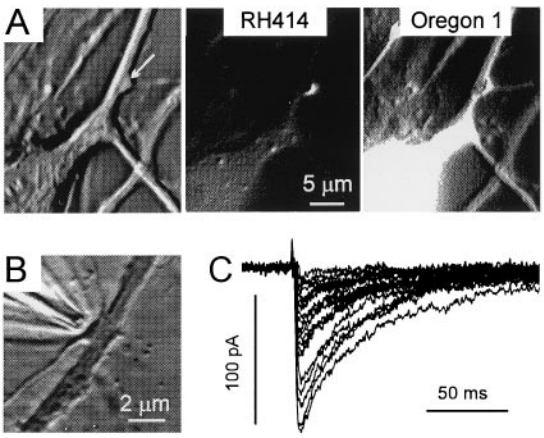

FIG. 1. Experimental conditions for recording responses to single-bouton activation. (*A*) Phase-contrast, RH414, and Org1 images at ×1,000 magnification (binning, 1 × 1, after modification by a shadow filter). The arrow points to the RH414-stained presynaptic bouton. (*B*) A stimulation pipette was positioned in close vicinity to a solitary bouton. (*C*) The postsynaptic response to activation of the bouton shown in *B* displayed a high degree of variability although stimulating currents were invariant throughout the experiment (1.5 μA, 2 ms, 0.2 s^{-1}). Traces after subtraction of averaged failure traces. Here and in all remaining figures, IPSCs were recorded at a holding potential of −70 mV. E_{Cl} was set at about −20 mV.

axis had an average length of 1.06 μm (SD = 0.41; $n = 50$). The RH414-labeled area comprised 5–10 pixels (binning 4 × 4).

All experiments were performed in boutons separated from their neighbors by more than 2 μm. Stimulating pipettes were positioned under visual guidance (Fig. 1*B*). Stationarity of synaptic transmission in the course of data acquisition was tested by comparing average response amplitudes in the first and second half of the experiment. We admitted a run-down of not more than 20% for stimulation frequencies between 0.1 and 0.2 s^{-1}. The number of trials (typically 150–200) was limited by bleaching of the Ca^{2+}-sensitive dye. Fig. 1*C* illustrates a response to stable single-bouton activation in the presence of tetrodotoxin. It can be seen that eIPSCs were stimulus-locked but highly variable in amplitude. Some of the responses were really large (>2 nS), especially if one considers that in these cultures 92% of the bouton profiles contained only one active zone (31) and quantal conductance changes were as low as 105–135 pS (32).

The large amplitude of single-bouton-activated eIPSCs raised the question of whether other boutons in the neighborhood were coactivated by the extracellular current pulse. This possibility was disregarded on the following grounds. First, the efficiency of stimulation was strongly dependent on the pipette position. A small (1- to 2-μm) displacement of the stimulation pipette resulted in the reversible disappearance of both eIPSCs and $[Ca^{2+}]_{pre}$ even if the strongest pulse (4 μA) was applied. Second, a stimulus-locked presynaptic Ca^{2+} signal occurred only in the depolarized bouton and was never detected in any other RH414-stained region within in the field of observation. Fig. 2 *A–C* illustrates that the evoked fluorescence change indeed was confined to the terminal in the immediate vicinity of the stimulating pipette.

An important issue was the potential influence of the depolarizing stimulus on the postsynaptic cell. The results presented in Fig. 2 *E* and *F* suggest that postsynaptic, voltage-activated conductances in the stimulated area, if at all present, were not detectable (below 50 pS). Similar results were obtained when adding 50 μM of bicuculline to SSS. Analysis of failure traces during application of Ca^{2+}-free solution (Fig. 2*E*) or in the SSS (Fig. 2*F*) showed that current relaxation after the stimulus was fairly fast. In the absence of an eIPSC, the time constants ranged from 1.5 to 2 ms ($n = 5$).

Another important task was to clarify whether the values of $[Ca^{2+}]_{pre}$ were affected by postsynaptic $[Ca^{2+}]$ transients. As illustrated in Fig. 2*D*, Ca^{2+} signals outside the RH414-stained area were much smaller (maximally 5–10%) than the presynaptic Ca^{2+} signal (50–60%). Together with the "dendritic Ca^{2+} test" mentioned in *Materials and Methods*, this result suggests that contamination of $[Ca^{2+}]_{pre}$ by the postsynaptic signal was not more than 5%.

Fig. 3*A* illustrates the temporal relationships between an individual $[Ca^{2+}]_{pre}$ transient and the corresponding eIPSC. In most cases $[Ca^{2+}]_{pre}$ reached its maximum during the second image, i.e., within 20 ms. The decay of $[Ca^{2+}]_{pre}$ was fitted by

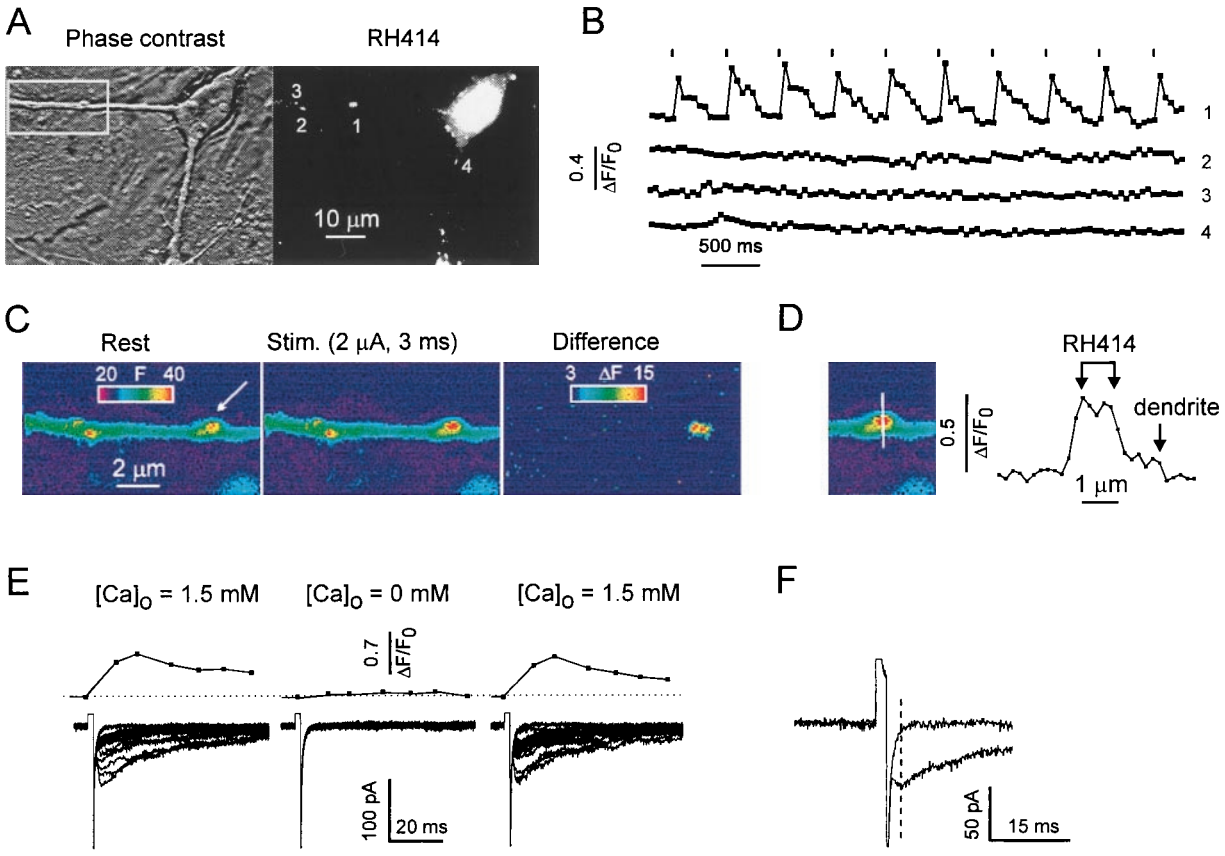

FIG. 2. Bouton activation by extracellular electrical stimulation is highly spatially selective. (*A*) Phase-contrast and RH414 image of an area comprising several boutons. (*B*) A train of short, depolarizing pulses (1.5 μA, 2 ms, 0.2 Hz) evoked a Ca^{2+} elevation only in the stimulated terminal (arrow). All other RH414-stained boutons in the view field lacked stimulus-locked Ca^{2+} transients (not all of them shown). Binning, 2 × 2; exposure time, 50 ms. (*C*) The same experiment. Enlarged image of the boxed area in *A*. The differential display illustrates selective activation of the stimulated bouton. (*D*) Profile of fluorescence change along a line through the stimulated bouton. Arrows point to the margins of the RH414-stained zone and the underlying dendrite. The stimulus (2 μA, 2 ms) increased the relative fluorescence by 50–60% in the bouton and by 5–10% in the dendrite. (*E*) Experiment with local application of Ca^{2+}-free solution. Stimulus intensity was 1.5 μA in standard extracellular $[Ca^{2+}]$ and was varied from 1.5 to 4 μA in Ca^{2+}-free solution. (*Upper*) Averaged $[Ca^{2+}]_{pre}$. (*Lower*) Superposition of postsynaptic responses. Note rapid and almost intensity-independent poststimulus relaxation in failure traces during the Ca^{2+}-free test. (*F*) Single, enlarged failure trace and eIPSC in response to identical stimuli (1.5 μA, 2 ms).

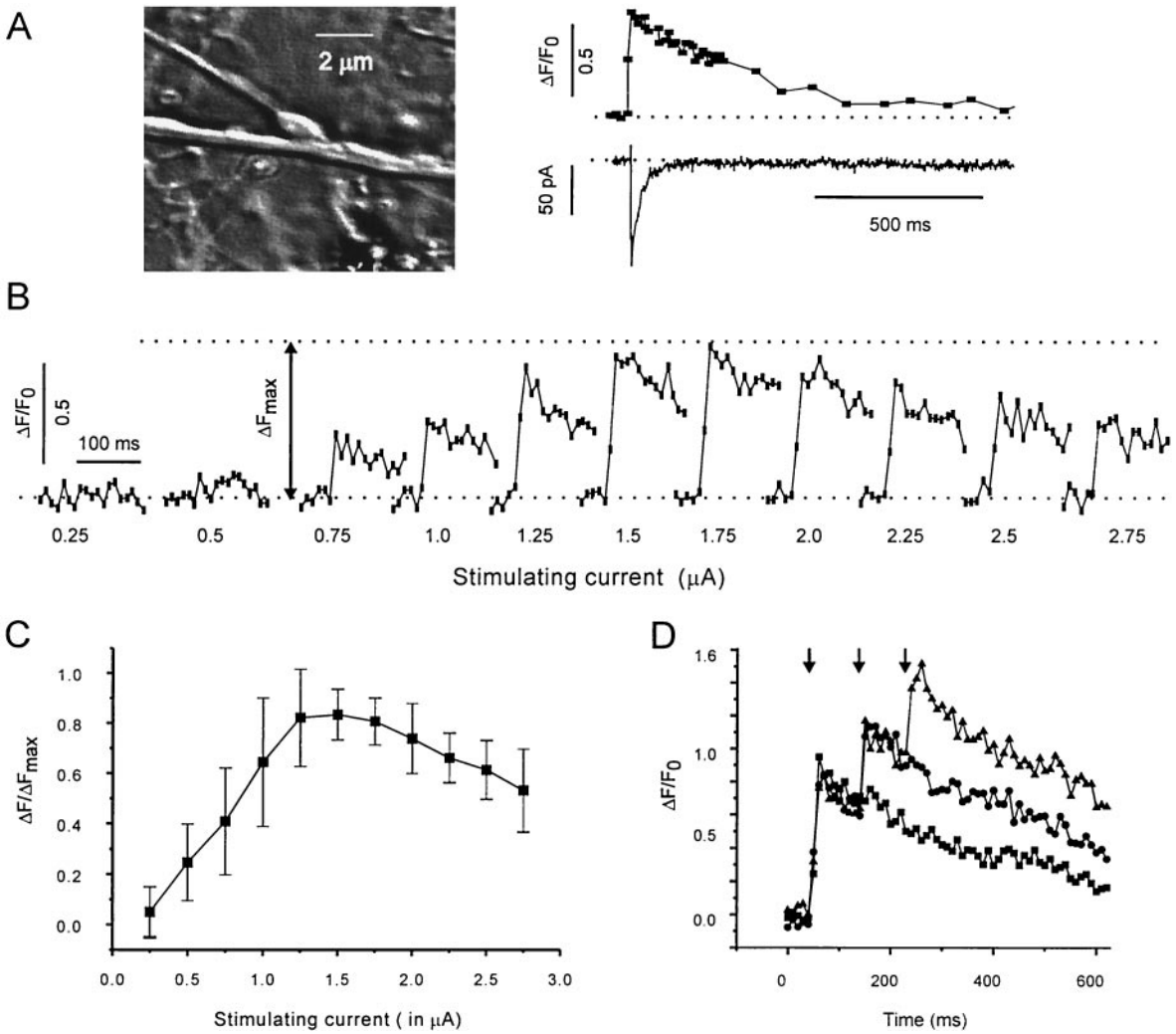

FIG. 3. Presynaptic Ca^{2+} signals in response to brief electrical stimulation of an isolated bouton. (*A*) Temporal relationship of an individual $[Ca^{2+}]_{pre}$ transient and the corresponding eIPSC. Depolarizing pulse: 2 μA, 1 ms. Note that the $[Ca^{2+}]_{pre}$ transient significantly outlasted the postsynaptic response. (*B*) Dependency of $[Ca^{2+}]_{pre}$ on stimulus intensity. Stimulus strength is given below each trace. Pulse duration: 3 ms. (*C*) Statistical representation of the same protocol as in *B* ($n = 7$). The recordings from each bouton were normalized by the maximal response (ΔF_{max}). Note that the amplitude of $[Ca^{2+}]_{pre}$ decreased when stimulus intensity exceeded 2 μA. (*D*) Test for indicator saturation. The bouton was stimulated with a series of 1–3 stimuli (3 ms at 0.1 s^{-1}). Pulse intensity (1.5 μA) was chosen to elicit maximal $[Ca^{2+}]_{pre}$ (see *C*). Note additional increase of fluorescence after the second and third pulse.

a single exponent function ($\tau = 390 \pm 80$ ms, $n = 30$). The amplitude of $[Ca^{2+}]_{pre}$ depended on the strength of the depolarizing current (Fig. 3 *B* and *C*). It can be seen that beyond a certain level of stimulus intensity (usually around 1.5 μA) the $[Ca^{2+}]_{pre}$ signal declined. Among other possibilities, this phenomenon could be explained by the decreasing driving force for the Ca^{2+} influx. Potential saturation of the Ca^{2+}-sensitive probe was tested by applying an increasing number of stimuli at short intervals. The pulse intensity was set to induce maximal Ca^{2+} elevation. These experiments (Fig. 3*D*) showed that the $[Ca^{2+}]_{pre}$ transient induced by the first pulse remained significantly below the maximal fluorescence level. Thus, single-pulse activation was unlikely to saturate the probe.

Fig. 4*A* illustrates the influence of $[Ca^{2+}]_{pre}$ on evoked GABAergic synaptic transmission. $[Ca^{2+}]_{pre}$ was varied by changing the size of the depolarizing current. Average eIPSCs were plotted against the fluorescence change. The latter was binned in steps of 0.05 arbitrary units. The power function fitting the data points of this experiment had an exponent of 3.4. The average from eight experiments was 2.9 ± 1.2 (range, 1.6–5.7). Regarding the relationship between postsynaptic responses and individual $[Ca^{2+}]_{pre}$, it should be pointed out that no eIPSC was ever seen in the absence of a $[Ca^{2+}]_{pre}$ transient, and, *vice versa*, all postsynaptic responses were accompanied by a significant increase of $[Ca^{2+}]_{pre}$. Thus, $[Ca^{2+}]_{pre}$ must be considered as a necessary condition for the generation of eIPSCs. But is it a sufficient condition as well? Fig. 4 *B* and *C* illustrates that this was not the case. In Fig. 4*C*, $[Ca^{2+}]_{pre}$ traces were selected to reach about the same maxima, but eIPSC amplitudes were quite different. Even a complete failure occurred in between two large eIPSCs.

Fig. 4 *B* and *C* illustrates that transmitter release retained its probabilistic character throughout the range of observed $[Ca^{2+}]_{pre}$ values. Because failures were not completely eliminated and maximal eIPSC amplitudes increased with larger $[Ca^{2+}]_{pre}$, elevation of $[Ca^{2+}]_{pre}$ resulted in a 3- to 4-fold increase in the amplitude range of postsynaptic responses.

The histograms of Fig. 5 *A* and *B* show the amplitude distributions of eIPSCs in more detail. By varying stimulus intensity, $[Ca^{2+}]_{pre}$ was set to its maximal level (Fig. 5*B*) and to about half of it (Fig. 5*A*). As expected, the failure rate decreased with higher $[Ca^{2+}]_{pre}$. The new finding is that higher $[Ca^{2+}]_{pre}$ shifted the eIPSC amplitude distribution toward larger values. However, increasing the stimulus intensity beyond the optimum for $[Ca^{2+}]_{pre}$ (see Fig. 3*B*) resulted in a decrease of eIPSCs (Fig. 5 *C–E*). Thus, in the higher-intensity

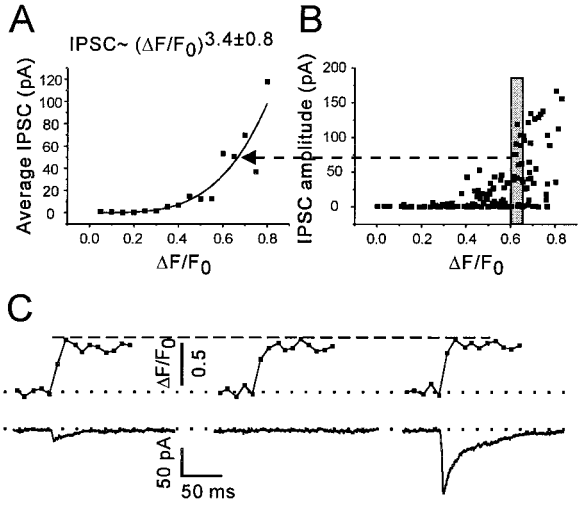

FIG. 4. $[Ca^{2+}]_{pre}$ determines not only the amplitude of average eIPSCs but also the range of eIPSC fluctuations. (*A*) The mean eIPSC amplitude increased with about the third power of $[Ca^{2+}]_{pre}$ (line). eIPSCs were averaged within $\Delta F/F_0$ bins. The $[Ca^{2+}]_{pre}$ bin width was set to 0.05. (*B*) Individual data points corresponding to the experiment shown in *A*. The gray bar delineates one bin of $[Ca^{2+}]_{pre}$. Fourteen individual data points were available for this level of $[Ca^{2+}]_{pre}$ (0.6–0.65), giving an eIPSC average and SD of 52.2 pA and 24.5 pA, respectively. All data are from the same bouton. Pulse duration: 1 ms. (*C*) eIPSCs fluctuate despite a similarity of $[Ca^{2+}]_{pre}$. Traces are presented in the order of acquisition. Data in *A* and *B* and in *C* were from different boutons.

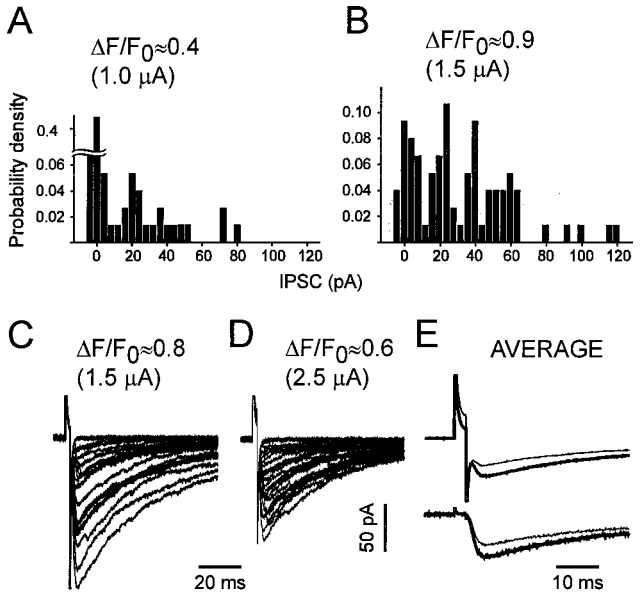

FIG. 5. In any given synapse, the largest eIPSC values obtained were associated with the highest $[Ca^{2+}]_{pre}$ values, but not the strongest stimulus intensity. (*A* and *B*) Normalized eIPSC histograms associated with smaller and larger $[Ca^{2+}]_{pre}$ in response to low-frequency stimulation (3 ms, 0.1 s^{-1}) at two different intensities. Pulses of 1 (*A*) and 1.5 (*B*) μA were applied to the same bouton in an alternating fashion. Bin width = 4 pA; $n = 75$. (*C* and *D*) Similar experiment in another bouton, but using stimulus intensities of 1.5 μA (*C*) and 2.5 μA (*D*). Pulse duration, 2 ms. *C* and *D* show 20 randomly selected traces each ($n = 70$). (*E*) Averaged traces corresponding to the experiment of *C* and *D*. Note that the stronger pulse (thin line) induced the smaller, averaged eIPSC. (*Lower*) The same traces as in *Upper* but after the artifact subtraction as described in *Materials and Methods*.

range, larger eIPSCs still were associated with larger $[Ca^{2+}]_{pre}$, but not with stronger depolarization ($n = 3$). The latter is an additional argument supporting our basic assumption that the stimulation activated only one bouton throughout the entire range of current intensities.

Taken together, these experiments show that single-bouton-activated eIPSCs are not at all confined to one stereotyped amplitude level. Even more, changes in eIPSC amplitudes could be produced experimentally. An increase of average eIPSCs in association with larger $[Ca^{2+}]_{pre}$ was the result of both a decrease in the failure rate and a shift toward larger eIPSC values. The simplest explanation for these results is that the number of vesicles simultaneously released from a single bouton can be greater than 1 and varies according to $[Ca^{2+}]_{pre}$.

DISCUSSION

High spatial and temporal resolution of signals in regions delineated by vesicle labeling has permitted us to investigate the relationship between pre- and postsynaptic responses to graded depolarization in small inhibitory boutons of the CNS. The work contains three main results: (*i*) average GABAergic eIPSCs displayed a power function dependency on $[Ca^{2+}]_{pre}$; (*ii*) at any given level of $[Ca^{2+}]_{pre}$, eIPSCs fluctuated; and (*iii*) larger $[Ca^{2+}]_{pre}$ transients resulted in larger maximal eIPSC amplitudes.

The relationship between $[Ca^{2+}]_{pre}$ and peak amplitudes of postsynaptic responses first was estimated on the basis of extracellular $[Ca^{2+}]$ changes. Studies in the neuromuscular junction and the squid giant synapse reported power relationships with an exponent between 2.5 and 3.8 (33–35). These numbers were confirmed later by studying the dependency of postsynaptic responses on presynaptic Ca^{2+} currents (12, 13) or $[Ca^{2+}]_{pre}$ (17, 18). Our data are in good agreement with the above results although the methods and preparations used were quite different. Considering that the number of active zones is about 5,000 in the squid giant terminal (2), about 500 in the frog neuromuscular junction (36), and probably no more then 5 in GABAergic boutons of the vertebrate CNS (15), one should conclude that the power law dependency of the mean postsynaptic response on $[Ca^{2+}]_{pre}$ applies equally well to large and small terminals. The present results can well be reconciled with the idea that the nonlinear dependency of GABA release reflects the summation of overlapping microdomains arising from multiple, clustered Ca^{2+} channels (17). However, several alternative explanations are possible, as discussed already by Augustine *et al.* (12).

Some degree of variability of postsynaptic responses is an inherent property of most central synapses (37). Part of this variability could be derived from the heterogeneity of individual contacts. Now we have shown that large eIPSC fluctuations persisted even in single boutons and in the trials selected to match each other with regard to $[Ca^{2+}]_{pre}$. Although larger $[Ca^{2+}]_{pre}$ elevations resulted in a significant decrease of the failure rate, failures of synaptic transmission appeared at all levels of $[Ca^{2+}]_{pre}$ observed. This indicates that a source of variability must exist downstream of the Ca^{2+} influx.

The nonlinear dependency of average eIPSCs on $[Ca^{2+}]_{pre}$ reflects not only a decrease in the fraction of failures but also a substantial increase in the amplitude of maximal eIPSCs. This finding contradicts the general assumption that in GABAergic synapses the quantal content varies only between 0 and 1 or, eventually, between 0 and 2 (see refs. 38 and 39 for a review). The present results are better reconciled with the experiments of Katz and Miledi (40), who studied endplate currents under conditions of K^+-channel blockade and estimated the relationship between evoked and miniature synaptic currents. They suggested that in the frog neuromuscular junction one active zone can release the contents of more than one vesicle if sufficient Ca^{2+} is available. However, additional experiments will be necessary to resolve the question of

whether, in CNS synapses, elevation of $[Ca^{2+}]_{pre}$ increases the number of quanta at one active zone or merely synchronizes the activity of several active zones in one terminal. Studies of evoked neurotransmission at the level of individual synapses in culture now provide further opportunities to determine the functional limits of single synapses, to clarify the experimental conditions for maximal release, and to find out to which extent molecular diversity contributes to response variability and heterogeneity in synapses formed under defined growth conditions.

We thank our colleagues Wolfgang Müller and Uwe Heinemann for helpful suggestions on the manuscript. The technical assistance of Mrs. Przezdziecki is highly appreciated. This study was supported by the Deutsche Forschungsgemeinschaft (Sonderforschungbereich 515, Project Grant B2 to R.G.).

1. Pumplin, D. W., Reese, T. S. & Llinás, R. (1981) *Proc. Natl. Acad. Sci. USA* **78,** 7210–7213.
2. Llinás, R., Sugimori, M. & Silver, R. B. (1992) *Science* **256,** 677–679.
3. Smith, S. J., Buchanan, J., Osses, L. R., Charlton, M. P. & Augustine, G. J. (1993) *J. Physiol. (London)* **472,** 573–593.
4. Landò, L. & Zucker, R. S. (1994) *J. Neurophysiol.* **72,** 825–830.
5. David, G., Barrett, J. N. & Barrett, E. F. (1997) *J. Physiol. (London)* **504,** 83–96.
6. Ravin, R., Spira, M. E., Parnas, H. & Parnas, I. (1997) *J. Physiol. (London)* **501,** 251–262.
7. DiGregorio, D. A. & Vergara, J. L. (1997) *J. Physiol. (London)* **505,** 585–592.
8. Yazejian, B., DiGregorio, D. A., Vergara, J. L., Poage, R. E., Meriney, A. D. & Grinnell, A. D. (1997) *J. Neurosci.* **17,** 2990–3001.
9. Augustine, G. J. & Neher, E. (1992) *Curr. Opin. Neurobiol.* **2,** 302–307.
10. Zucker, R. S. (1996) *Neuron* **17,** 1049–1055.
11. Neher, E. (1998) *Neuron* **20,** 389–399.
12. Augustine, G. J., Charlton, M. P. & Smith, S. J. (1985) *J. Physiol. (London)* **369,** 163–181.
13. Borst, J. G. G. & Sakmann, B. (1996) *Nature (London)* **383,** 431–434.
14. Harris, K. M. & Sultan, P. (1995) *Neuropharmacology* **34,** 1387–1395.
15. Sur, C., Triller, A. & Korn, H. (1995) *J. Comp. Neurol.* **351,** 247–260.
16. Regehr, W. G. & Tank, D. W. (1991) *J. Neurosci. Methods* **37,** 111–119.
17. Mintz, I. M., Sabatini, B. L. & Regehr, W. G. (1995) *Neuron* **15,** 675–688.
18. Wu, L. G. & Saggau, P. (1994) *J. Neurosci.* **14,** 645–654.
19. Ryan, T. A., Reuter, H., Wendland, B., Schweizer, F. E., Tsien, R. W. & Smith, S. J. (1993) *Neuron* **11,** 713–724.
20. Grantyn, R. & Veselovsky, N. S. (1998) in *Central Synapses: Quantal Mechanisms and Plasticity*, eds. Faber, D. S., Korn, H., Redman, S. J., Thompson, S. M. & Altman, J. S. (Human Frontiers Science Program, Strasbourg), pp. 108–115.
21. Katz, B. & Miledi, R. (1967) *J. Physiol. (London)* **192,** 407–436.
22. Lavidis, N. A. & Bennett, M. R. (1993) *J. Auton. Nerv. Syst.* **43,** 41–50.
23. Vautrin, J., Schaffner, A. E. & Barker, J. L. (1993) *Hippocampus* **3,** 93–102.
24. Liu, G. & Tsien, R. W. (1995) *Nature (London)* **375,** 404–408.
25. Vogt, K., Lüscher, H.-R. & Streit, J. (1995) *Eur. J. Physiol.* **430,** 1022–1028.
26. Bekkers, J. M. & Stevens, C. F. (1995) *J. Neurophysiol.* **73,** 1145–1156.
27. Stevens, C. F. & Tsujimoto, T. (1995) *Proc. Natl. Acad. Sci. USA* **92,** 846–849.
28. Burnod, Y. & Korn, H. (1989) *Proc. Natl. Acad. Sci. USA* **86,** 352–356.
29. Perouansky, M. & Grantyn, R. (1989) *J. Neurosci.* **9,** 70–80.
30. Kraszewski, K. & Grantyn, R. (1992) *J. Neurobiol.* **23,** 766–781.
31. Warton, S. S., Perouansky, M. & Grantyn, R. (1990) *Dev. Brain Res.* **52,** 95–111.
32. Kraszewski, K. & Grantyn, R. (1992) *Neuroscience* **47,** 555–570.
33. Katz, B. & Miledi, R. (1970) *J. Physiol. (London)* **207,** 789–801.
34. Lester, H. A. (1970) *Nature (London)* **227,** 493–496.
35. Dodge, F. A., Jr., & Rahamimoff, R. (1967) *J. Physiol. (London)* **193,** 419–432.
36. Torri-Tarelli, F., Grohovatz, F., Fesce, R. & Ceccarelli, B. (1985) *J. Cell Biol.* **101,** 1386–1399.
37. Korn, H. & Faber, D. S. (1987) in *Synaptic Function*, eds. Edelman, G. M., Gall, W. E. & Cowan, W. M. (Wiley, New York), pp. 57–108.
38. Arancio, O., Korn, H., Gulyas, A., Freund, T. & Miles, R. (1994) *J. Physiol. (London)* **481,** 395–405.
39. Auger, C., Kondo, S. & Marty, A. (1998) *J. Neurosci.* **18,** 4532–4547.
40. Katz, B. & Miledi, R. (1979) *Proc. R. Soc. London Ser. B* **205,** 369–378.